C.P. No. 813

MINISTRY OF AVIATION

AERONAUTICAL RESEARCH COUNCIL

CURRENT PAPERS

Theoretical Investigation of Some Basic Assumptions of Schlichting's Singularity Method of Cascade Analysis

By

R.I. Lewis and G.A. Pennington

LONDON: HER MAJESTY'S STATIONERY OFFICE

1965

SEVEN SHILLINGS NET

Theoretical Investigation of Some Basic Assumptions of Schlichting's Singularity Method of Cascade Analysis

- By -
R. I. Lewis and G. A. Pennington

Communicated by Prof. J. H. Horlock

C.P. No. 813

September, 1964

SUMMARY

The accuracy of Schlichting's kinematic source flow equation has been investigated for an isolated symmetrical aerofoil. Studies are presented also of the suitability of the Glauert series for representing profiles by source/vortex distributions. Influence of data rounding off error upon profile analysis with large numbers of control points has been examined, and importance of data accuracy and smoothness stressed. An estimation of the optimum number of control points has been made for a typical profile. A method of initial data processing to ensure a valid computation has been suggested.

1./

Replaces A.R.C. 26 159

1. INTRODUCTION

Of the wide variety of published cascade analyses, Schlichting's method of singularities,[1] applicable to incompressible inviscid flow through cascades of thin low-cambered aerofoils, is probably the most suited for extensive use. The method is rapid, well suited to digital computation and gives good agreement with experiment for a wide range of stagger and solidity.

Following the established basis of thin aerofoil theory, Schlichting represents the blade profiles as streamlines generated by source and vortex distributions $q(x)$ and $\gamma(x)$ located in a uniform stream of velocity W_∞. The source distribution produces profile thickness while the vortex distribution induces curvature of the flow which in theory is matched to the curvature of the camber line, Figure (1). These singularity distributions are expanded as Fourier series with an additional special term.

$$q(x) = 2U_\infty \left\{ B_0 \left(\mathrm{Cot}\tfrac{\phi}{2} - 2\mathrm{Sin}\phi\right) + B_2 \mathrm{Sin}2\phi + \text{etc.} \right\} \quad (1)$$

$$\gamma(x) = 2U_\infty \left\{ A_0\mathrm{Cot}\tfrac{\phi}{2} + A_1\mathrm{Sin}\phi + A_2\mathrm{Sin}2\phi + \text{etc.} \right\} \quad (2)$$

where

$$\frac{x}{l} = \frac{1}{2}(1 - \mathrm{Cos}\phi) \quad (3)$$

U_∞ is the component in the x or chord direction, Figure (1) of the vector mean velocity W_∞. l is the chord length.

The term containing $\mathrm{Cot}\frac{\phi}{2}$ has a special significance in each case. In the source series this term, in the absence of others, produces the thickness of a Joukowsky profile[1]. This term is thus usually important since it produces the general characteristics of an aerofoil, namely a blunt nose and sharp trailing edge. The Fourier series provides further control over the profile shape.

In the vortex series the first term alone corresponds to the vorticity distribution of a flat plate with incidence. The remaining terms of the Fourier series are required for producing curvature to match the camber line. If the cascade operates with shock-free inflow, by definition, the stagnation point is located on the camber line at the leading edge. Ao is then zero. For all other incidences a vortex singularity exists at x = o producing the suction peak which is always to be found at off-design inlet angles.

The simplicity of Schlichting's analysis resulted from a number of restrictive assumptions. The major simplification was to locate the singularities on the chord line rather than the camberline. This reduced analytical complexity but restricted the allowable range of camber over which the theory may be safely applied. This assumption has not been investigated in great detail here but some indication of the range of validity has been given in the latter part of the report by a comparison of this theory with the exact theory of Merchant and Collar applied to cascades of 70° and 120° of camber. The authors are indebted to Mr. P. Gostelow of Liverpool University for his cooperation in deriving these exact solutions.

Further assumptions were made by Schlichting in deriving the kinematic equation which relates source strength to profile thickness. The main purposes of this investigation were to examine the accuracy of the simplified equation and to study the adaptability of the source Fourier series for matching arbitrary profiles. The project was extended further on the basis of the conclusions that accurate smooth profile data were essential if large numbers of control points were to be used. To this end a method of input data processing was devised which ensures a valid analysis.

The contents of the report may be summarised as follows.

Section 2.

Derivation of kinematic flow equations.

Section 3.

Investigation of the accuracy of the kinematic source flow equation by comparison with an exact solution.

Section 4.

Study of the adaptability of the source series when using large numbers of control points; especially the importance of specifying accurate smooth input data, analysis of an unusual profile and estimation of the optimum number of control points.

Section 5.

Data processing to ensure the best representation of a given profile.

Section 6.

Comparison of the performance of cascades with cambers of 70° and 120°, as predicted by Schlichting's theory and the exact theory of Merchant and Collar.

2. KINEMATIC FLOW EQUATIONS

The Kinematic flow equation of particular interest here is the one which relates $q(x)$ to the profile thickness y_d. If the continuity equation is written for the small area ABCD of the symmetrical profile illustrated in Figure (1) we have

$$\tfrac{1}{2}q(x)dx = (U_\infty + u + \frac{du}{dx} \cdot dx)(y_d + \frac{dy_d}{dx} \cdot dx) - (U_\infty + u)y_d \quad (4)$$

Velocities are defined in Figure (1)a.

This equation is not exact since it neglects the variation of u with y. For thin profiles this is likely to be a good assumption apart from the leading and trailing edge regions where a more detailed investigation of the assumption would be valuable.

The profile slope, on rearranging terms, is

$$\frac{dy_d}{dx} = \frac{\tfrac{1}{2}q(x) - y_d\frac{du}{dx}}{U_\infty + u + \frac{du}{dx} \cdot dx} \quad (4)a$$

Schlichting made the further assumption that $\frac{du}{dx}$ is small enough to be neglected also which then results in the more approximate equation.

$$\frac{dy_d}{dx} = \frac{q(x)}{2(U_\infty + u)} \quad (5)$$

It is possible, following Schlichting, to simplify this equation still further for the case of very thin isolated profiles for which $u \ll U_\infty$. The equation then reduces to

$$\frac{dy_d}{dx} = \frac{q(x)}{2\,U_\infty} \quad (6)$$

which as the special appeal that it is directly integrable yielding equation (10) below.

The vortex kinematic flow equation states that the total induced velocity must have no component normal to the camber line. Referring to Figure (1)b this results in the equation.

$$\frac{dy_s}{dx} = \frac{V_\infty + v}{U_\infty + u} \quad (7)$$

where U_∞ and V_∞ are the components, parallel and normal to the chord line, of the vector mean velocity W_∞ . u and v are the velocity components of the flow induced by the singularities. If it is assumed, as is reasonable, that $v_q \ll v_\gamma$ and also that $u \ll U_\infty$ this equation approximates to

$$\frac{dy_s}{dx} = \frac{V_\infty + v_\gamma}{U_\infty} \tag{8}$$

where v_γ is given by

$$v_\gamma = \frac{1}{2\pi} \int_{x'=0}^{x'=1} \left\{ \frac{\gamma(x')}{x' - x} \right\} dx' \tag{9}$$

Direct integration of equations (6) and (8) using equations (1), (2) and (9) yields

(10)

$$\frac{y_d}{l} = \tfrac{1}{2}B_0 \left(\mathrm{Sin}\emptyset + \tfrac{1}{2}\mathrm{Sin}2\emptyset\right) + \frac{1}{12} B_2(3\mathrm{Sin}\emptyset - \mathrm{Sin}3\emptyset) + \frac{1}{16}B_3(2\mathrm{Sin}2\emptyset - \mathrm{Sin}4\emptyset) + \ldots \text{etc.}$$

(11)

$$\frac{y_s}{l} = \tfrac{1}{8}A_1 (1 - \mathrm{Cos}2\emptyset) + \frac{1}{12}A_2(\mathrm{Cos}\emptyset - \mathrm{Cos}3\emptyset) - \frac{1}{16}A_3(1 - 2\mathrm{Cos}2\emptyset + \mathrm{Cos}4\emptyset) + \ldots \text{etc.}$$

These equations were used for the studies described in sections (4) and (5),

From this preliminary background theory we proceed to the various investigations.

3. COMPARISON OF APPROXIMATE AND EXACT THEORY FOR FLOW PAST A SYMMETRICAL PROFILE

In this section a comparison is made between the actual profile generated by a given source distribution in a uniform stream U and the analysis of this profile by Schlichting's method using equation (5). The simplest case is considered, namely that of an isolated aerofoil, or cascade of infinite pitch. The complication of interference from adjacent blades is then removed. The exact theory used here actually required the implementation of numerical techniques for integration and was in practice subject to error from this source. By repeating the integrations with decreasing increments it was possible to check successive solutions and to ensure that errors were negligible in comparison with the analytical errors under investigation. Details of the exact theory are contained in Appendix II. The derivation of the approximate solution and the general prodedure of the investigation were as follows.

An equation analogous to (9), but for the velocity induced by the source distribution, is

$$u_q = \frac{1}{2\pi} \int_{x'=0}^{x'=1} \left\{ \frac{q(x')}{x - x'} \right\} dx' \qquad (12)$$

This equation may be integrated to yield

$$u_q = U_\infty \left\{ B_o(1 + 2\text{Cos}\phi) - B_2\text{Cos}2\phi - B_3\text{Cos}3\phi + \text{etc.} \right\} \qquad (13)$$

Remembering also equation (1), equation (5) now becomes

$$\frac{dy_d}{dx} = \frac{B_o(\text{Cot}\phi/2 - 2\text{Sin}\phi) + B_2\text{Sin}2\phi + B_3\text{Sin}3\phi + \text{etc.}}{1 + B_o(1 + 2\text{Cos}\phi) - B_2\text{Cos}2\phi - B_3\text{Cos}3\phi + \text{etc.}} \qquad (14)$$

The investigation proceeded in three stages dealt with in the following subsections.

3.1 Derivation of a set of realistic coefficients B_o, B_2, B_3, for a three term series.

3.2 Computation of the induced profile and surface velocity using exact theory.

3.3 Analysis of the exact profile by Schlichting's method yielding the approximate source distribution and surface velocity.

3.1 Derivation of a Typical Source Distribution

In order to derive a set of coefficients B_o, B_2, B_3 which would for sure produce a realistic aerofoil, the first step was to choose a typical aerofoil and to match it by Schlichting's method using a simplified form of equation (14) corresponding to the approximate kinematic equation (6).

$$\frac{dy_d}{dx} = B_o(\text{Cot}\phi/2 - 2\text{Sin}\phi) + B_2\text{Sin}2\phi + B_3\text{Sin}3\phi + \text{etc.} \qquad (15)$$

By matching the profile slope at the three control points $x/_1 = 3/4,\ 7/12,\ 11/12$ recommended by Schlichting, a set of three simultaneous equations in B_o, B_2, B_3 was obtained. The solution yielded the values

$$B_o = 0.081307$$
$$B_2 = 0.111628$$
$$B_3 = 0.035256$$

for which the corresponding distribution is shown in Figure (2), curve (a).

3.2 Derivation of Induced Profile by Exact Theory

For this source distribution the corresponding profile was computed by exact theory as outlined in more detail in Appendix II. The resulting profile is shown in Figure (3), curve (a), plotted to an expanded y_d scale.

3.3 Analysis of Exact Profile by Schlichting's Method

Having obtained now a profile and its source distribution, the accuracy of Schlichting's approximate kinematic equation (5) was checked by subjecting this profile to an analysis identical to that described in Section 3.1, but making use of the more exact equation (14) for the profile slope corresponding to Schlichting's equation (5).

The surface velocity W was computed, remembering equation (13), by the introduction of Riegel's factor [1].

$$W = \frac{U_\infty + u}{\sqrt{1 + (y'_d)^2}} \qquad (16)$$

The source distribution and profile derived by this procedure are compared with the exact analysis in Figures (2) and (3). The profile could not be derived here by direct integration of equation (14). Instead the slope was computed for a large number of chordwise positions and the profile determined by numerical integration from the trailing edge forwards. Because of the infinite slope at the leading edge this was an unsuitable starting point for the integration.

The coefficients thus determined were

$$B_o = 0.072546$$
$$B_2 = 0.093271$$
$$B_3 = 0.013467$$

The approximate profile matched the exact one very closely, Figure (3), although in this case the derived source distribution was on average about 85% of the true value. The good profile matching is not surprising when it is remembered that the profile shape is related to a three term source series through the more approximate equation (15). Indeed such good agreement of the profiles was the original deliberate intention in order that the error in q(x) could be isolated from the error in profile matching.

The surface velocity and pressure distributions yielded by the two theories are compared in Figure (4) and (5). An encouraging measure of agreement was obtained for this profile which has a fairly large maximum thickness of 14.4 per cent of the chord. The fractional error in velocity and pressure is less than that of the derived source strength because the source-induced velocity has finally to be added to U_∞ which is at all points

at least five times the magnitude of the source velocities. In other words a first order error in q(x) leads only to a second order error in velocity and pressure.

This investigation has demonstrated that for a typical aerofoil, Schlichting's kinematic source flow equation is accurate enough for practical purposes.

3.4 Position of the Leading Edge.

It is well known that a source in a uniform stream generates a parabolic streamline separating the mainstream from the source flow, with a stagnation point upstream of the source. It is shown in Appendix II that the series source distribution generates a profile whose leading edge coordinate is located just upstream of x = 0 at a position given by

$$\sqrt{-x=} \frac{B_0}{1 + 3B_0 - B_2 - B_3} - - \frac{5B_0 - 4B_2 - 6B_3}{1 + 3B_1 - B_2 - B_3} \quad x$$

For the aerofoil under investigation

$$x/_1 = - 0.005$$

which is negligible for practical purposes

4. INFLUENCE OF DATA ACCURACY, PROFILE SHAPE, AND NUMBER OF CONTROL POINTS UPON MATCHING.

This section is concerned with the accuracy with which an aerofoil may be represented by the source series. Particular attention is concentrated on the advantage or otherwise of using an extended series with many control points for the purpose of obtaining closer matching. Light is shed upon the importance of beginning with accurate smooth data when using large numbers of control points. A restricted study has also been made to estimate the optimum number of control points for obtaining the best matching of a typical aerofoil.

This investigation could be viewed alternatively as a study of the adaptability of the particular series chosen for representing functions with the general characteristics of aerofoil thickness distribution. For this reason, the simplest kinematic equation (6) was adaquate to illustrate this point. A further computational advantage was gained in that the profile was then represented analytically by equation (10), and the profile slope by equation (15). The surface velocity was computed by equation (16).

4.1 Importance of Data Accuracy with Many Control Points

Three calculations were made of flow past a given profile with 19 control points. Data was supplied to eight, four and three significant places respectively, in order to study the influence of data accuracy upon the efficacy of Schlichting's method.

The profile chosen for this purpose was generated by a three term series using equation (10), and is shown as curve (a) in Figure (7). It was expected therefore ideally that analysis of this profile with 19 control points would yield coefficients B_n of zero magnitude for $n > 3$ and identical coefficients for $n < 3$. As the original profile was given to eight significant figures, this procedure represents the best working accuracy within the computing facilities, but of course an accuracy far in excess of that which is usually practicable. The coefficients are compared in columns 1 and 2 of the table below.

Table of Coefficients for Source Series

Coefficient	Actual Value	Derived Values			
		8 Sig.Fig.	4 Sig.Fig.	3 Sig.Fig.	Modified Profile
B_o	+.08929	+.08938721	+.01227	-2.03680	-49.61142
B_2	+.10417	+.10403869	+.21420	+3.20245	+66.41216
B_3	+.03422	+.03404535	+.18591	+4.22084	+97.89990
B_4		-.00008599	+.07043	+2.05419	+37.04083
B_5		-00016487	+.14285	+3.94196	+92.18334
B_6		-.00005200	+.03878	+1.20631	+14.60056
B_7		-.00014320	+.12525	+3.45599	+80.77051
B_8		-.00002236	+01684	+ .60021	+ .56769
B_9		-.00011359	+.09953	+2.74549	+64.01240
B_{10}		-.00000887	+.00435	+ .23139	- 5.65969
B_{11}		-.00007902	+.06942	+1.91463	+44.50483
B_{12}		-.00000011	-.00077	+ .05279	- 6.20496
B_{13}		-.00004376	+.04078	+1.12344	+25.87339
B_{14}		-.00000005	-.00158	- .00559	- 3.90033
B_{15}		-.00001995	+.01890	+ .52030	+11.69935
B_{16}		+.00000106	-.00084	- .00988	- 1.52059
B_{17}		-.00000560	+.00618	+ .16938	+ 3.67146
B_{18}		+.00000059	-.00021	- .00296	- .30429
B_{19}		-.00000091	+.00108	+ .02932	+ .60093

The coefficients in column 1 for three control points and in column 2 for nineteen control points, agree to only three decimal places despite eight significant figures of accuracy of initial data. This is due partly to rounding off errors during the solution of the simultaneous equations and partly to the added necessity for matching with high order terms the rounding off error in the eighth decimal place of the original data.

In order to assess which was the more important of the above causes, two further calculations were made of the same profile, but with the coordinates rounded off to four and to three significant figures representing the usual order of accuracy encountered in practice. It will be observed that the coefficients, tabulated on the previous page, in neither case bear any resemblance to the original ones. On the contrary, some high order coefficients are greater in magnitude than B_0, B_2, and B_3. This confirms that these high order terms are required to match the surface ripple of amplitude equal to the rounding off error.

The singularity distributions, profiles and pressure distributions for these cases are shown in Figures (6), (7) and (8). Curves (a) are for the original three term series. Curves (b), (c) and (d) show results for eight, four and three significant figures.

The singularity distribution with eight significant figures differed by a negligible amount from the original, Figure (6). Case (c) agreed quite well over the central range but large oscillations occured at the extremities. These errors increased and extended further into the mid-chord region for case (d).

The corresponding profiles, Figure (7), were derived from equation (10). As before cases (a) and (b) differed by a negligible amount. For case (c), the profile shape was correct over the central range but displaced slightly. The further reduction of accuracy in case (d) produced a remarkable result. Although as before the general profile shape was retained over the central range, the vertical shift was increased to such an extent that the coordinates assumed large negative values over the whole chord. The high order terms had introduced such large oscillations at the extremities of the range as to introduce a large net sink strength upstream of the position where the profile slope is more accurately matched. The profile results are of course meaningless. With such a singularity distribution in reality no profile would exist. Streamlines would enter the chord line near the leading edge, and leave towards the trailing edge. The computed pressure distributions, Figure (8), exhibited similar tendencies. In this case the pressure distribution with four significant figures was quite close to the original.

From these calculations it is evident that accurate presentation and smoothness of data is vital. Smoothness of data and suitability to the matching series was ensured by choosing a profile corresponding to a three term series. For this special profile a reasonable prediction of pressure distribution was obtained with four significant figures. On the other hand no advantage was gained by matching the profile at 19 control points. Further improvement would require greater accuracy of specified data.

4.2 Matching an Unusual Profile

As already mentioned, the profile dealt with in section (4.1) was carefully chosen to ensure a favourable thickness distribution devoid of characteristics which would require higher order terms of the series. For the next study a bulge was added onto this profile, Figure (7)e, near to the trailing edge in order deliberately to introduce dominant high order terms. The profile was then matched at 19 control points resulting in the coefficients given in the last column of the table. The singularity distribution, profile and pressure distribution are plotted in Figures (6) to (8), curves (e).

The oscillations of singularity strength at the extremities of the range were even greater than case (d). Once again the general profile shape including the bulge was quite well matched, though displaced a considerable distance in the negative y_d direction.

It is quite clear from this study that the method must be applied with care. The adoption of a large number of control points is not the irrefutable remedy for dealing with unusual profiles. In fact the same might be said for profiles which appear reasonable, but which nevertheless require large high order terms. This is further illustrated in the next section which deals with such a profile analysed for 3, 5 and 10 control points.

4.3 Estimation of Optimum Number of Control Points for a Typical Aerofoil

The purpose of this investigation was to estimate for a typical aerofoil and optimum number of control points. The profile was analysed with 3, 5 and 10 control points. Data was specified to four significant figures. The simplified equation (10) was used. Results are shown in Figures (9) to (11).

The singularity distribution, which is equal, by equation (6), to $2U_\infty y_d'$ was computed in between control points, Figure (9). Progressive increase in accuracy of matching was obtained.

The computed profile, Figure (10), with 10 control points matched the original closely over most of the chord including the curvature at the trailing edge. The latter, however, introduced high order terms which

caused a reversal of profile curvature at about 7 per cent of the chord. This produced a kink in the pressure distribution at the same position, Figure (11). With 5 control points it was not possible to follow the trailing edge curvature. In consequence the derived profile was parallel to the original but displaced in the y_d direction by about 6 per cent of the chord. The pressure distributions suggest that this was an acceptable error. Agreement was close over the mid-chord region where the 10 control point case gave accurate profile representation. The suction peak corresponding to ideal flow around the curved trailing edge was of course eliminated. In fact an advantage has been gained here by reducing the number of control points. In actual fluid flow past the trailing edge, this suction peak is not found because of the cushioning effect of the boundary layer which has grown to its maximum thickness at the trailing edge. Correction of the original profile by addition of the displacement thickness would be more representative of the ideal fluid situation we wish to match. Furthermore, the fluid in practice separates from the trailing edge as from a bluff body, and leaves the aerofoil in a direction which is probably close to the camber line. The solution with 5 control points may well be much more representative of the true viscous flow at the trailing edge. Added to this, the elimination of the reversal of curvature near the leading edge commends the 5 control point case.

With three control points a much inferior profile match was obtained. This was reflected in the pressure distribution also.

From this investigation it was concluded that a good representation of an average profile could be obtained with 5 control points. With less control points a smooth profile was obtained, but the general shape was not adequately matched. With more control points the general shape was matched closely at the expense of the leading edge where the beginnings of profile undulations were observed. In addition, the close matching of the trailing edge curvature with 10 control points did not necessarily represent the real viscous flow. In fact the 5 control point case was considered to be more probably equivalent in character because of the smooth decelerating flow from the trailing edge.

5. DATA PROCESSING TO GIVE BEST MATCHING.

It is possible to overcome the difficulties outlined in section (4) by processing the input data. A method which has been used with success[2] is as follows. As the source series is finally to be used, it is logical to begin by representing the original profile by a function which it is certain can be closely matched. Equation (10) for the thickness and equation (11) for the camber are the obvious choice. These series, truncated to the same number of terms as will be used in the cascade analysis, are then matched to the given aerofoil by the method of least squares.

This method has been tried out on a compressor cascade 10C2/20C50 using three control points. The original, processed and final integrated profiles are compared in Figure (12), where y_d is plotted on an expanded scale. Three terms were sufficient in this case to represent the C2 profile and circular arc camber line with good accuracy. The processed profile was close to the original and the final integrated profile derived from the actual cascade analysis agreed with the original to well within 1 per cent of the chord at all points.

6. HIGH CAMBER CASCADES

Schlichting's assumption that the singularities are located on the chord line is the one most open to question. A full investigation was beyond the scope of this project. The comparisons presented here between exact and approximate theories do however give an indication of the range of validity of this assumption. The profiles chosen, shown in Figure (14), have cambers of 70° and 120° respectively. The 70° cambered profile is very similar to 10C4/70C50. Also shown in Figure (14) are the integrated profiles derived from the computed singularity strengths which show that the Schlichting analysis was obtaining a good profile match. Three control points were used.

The 70° camber profile was analysed with zero stagger, a pitch/chord ratio of 0:9 and for inlet angles of +35° and -35°. For both cases the computed pressure distributions, Figure (15), were in very good agreement. The computed outlet angles were as follows:

Inlet Angle	α_2 Merchant and Collar	α_2 Schlichting 3 control points
+ 35°	23.80°	20.28°
- 35°	24.84°	22.57°

This can be considered as good agreement considering the large deflection of the cascade.

The 120° cambered blade was analysed for zero stagger and a pitch/chord ratio of 0.59. In this case, Figure (16), the pressure distributions bore some resemblance over the first 50% of chord but differed strongly over the remainder of the span. The outlet angles were as follows;

$\alpha_2 = 51.17°$ Merchant & Collar

$= 46.32°$ Schlichting

Thus although the the deflection was predicted to within 5 per cent, Schlichting's theory did not give a satisfactory prediction of pressure distribution for this case of very high camber.

7. SUMMARY OF CONCLUSIONS

The main conclusions may be summarised as follows:-

(a) It has been demonstrated that for a typical aerofoil Schlichting's kinematic source flow equation is accurate enough for normal profiles. Source strength is 15 per cent too small, but pressure is given to within 4 per cent of the main stream dynamic head.

(b) The streamline representing the profile cuts the chord at a position of approximately $\frac{1}{2}$ per cent of chord upstream of the assumed profile leading edge.

(c) Accurate presentation and smoothness of data has been found to be vital.

(d) The adoption of large numbers of control points will not ensure better matching of unusual profiles. On the contrary severe surface undulations and even complete breakdown of the matching process can occur. On the other hand, the method has proved eminently suitable for practical profiles which are known to be good aerodynamically.

(e) The optimum number of control points for a typical profile was 5. This can only be regarded as a guide. A greater number leads to surface undulation and less representative flow at the trailing edge. Having less control points restricts the matching accuracy over the central chord region.

(f) These difficulties can be overcome by initial data processing to ensure accurate input data of a form acceptable to the matching process. Most of the restrictions to profile matching resulting from use of a truncated series are imposed in this initial step. A valid Schlichting's analysis is then ensured.

(g) The method proved accurate enough for a cascade with 70° of camber. Pressure distributions are probably inaccurate above this, although fluid outlet angle was predicted to within 3° for the case considered here with 120° of camber.

REFERENCES

(1) H. Schlichting — Calculation of the frictionless incompressible flow for a given Two-dimensional Cascade (Direct Problem). NACA/TIL Misc. 128. Translation from VDI - Fors chungsheft 447, Edition B, Vol.21, 1955.

(2) G.A. Pennington — Data Smoothing and Differentiation for Schlichting's Calculations. Report No. W/M(4A)p.152, 1.11.63. English Electric Co. Ltd., Whetstone.

(3) Merchant, W and Collar, A.R. — "Flow of an ideal fluid past a cascade of blades". Part II. A.R.C. R & M. No. 1893 (1941)

ACKNOWLEDGMENTS

The author is indebted to Mr. P. Gostelow of Liverpool University for computing the exact solutions by the method of Merchant and Collar. He is also grateful to the management of the English Electric Co. Ltd., Whetstone for permission to publish this work.

APPENDIX I

NOTATION

x		Direction parallel to chord line.
y		Direction perpendicular to chord line.
y_d		Profile thickness.
y_s		Camber line coordinate.
l		Chord.
ϕ		Variable of chord defined $\frac{x}{l} = \frac{1}{2}(1 - \cos\phi)$
$q(x)$		Source strength per unit length.
$\gamma(x)$		Vortex strength per unit length.
$Q(x)$	$= \int_0^x \frac{q(a)}{2U}\, da$	
W_∞		Vector mean velocity.
U_∞		Component of W_∞ in x direction.
V_∞		Component of W_∞ in y direction.
ψ		Stream Function.
$u = \frac{\partial \psi}{\partial y}$		Singularity Velocity perturbation in x direction.
$V = -\frac{\partial \psi}{\partial x}$		Singularity Velocity perturbation in y direction.
u_q	$= \frac{1}{2\pi} \int_{x'=0}^{x'=1} \left\{ \frac{q(x')}{x - x^1} \right\} dx'$	Velocity perturbation due to source distribution.
v_γ	$= \frac{1}{2\pi} \int_{x'=0}^{x'=1} \left\{ \frac{(x')}{x' - x} \right\} dx'$	Velocity perturbation due to vortex distributio

APPENDIX II

Derivation of profile induced by a source distribution in a Uniform Stream

The stream function is defined by

$$u = \frac{\partial \psi}{\partial y}, \qquad v = -\frac{\partial \psi}{\partial x} \tag{2.1}$$

The profile in Figure (13) is to be represented by the streamline $\psi = 0$ generated by the source distribution $q(x)$ in a uniform stream of velocity U.

Since ψ is a function of x and y

$$d\psi = \frac{\partial \psi}{\partial y} \cdot dy + \frac{\partial \psi}{\partial x}\, dx$$

Hence for two points on the profile $\psi_A - \psi_B = \int_B^A u\,dy -$

$$\int_B^A v\,dx = 0 \tag{2.2}$$

If the integration is taken along the contour BpqrA for example where the y co-ordinate ϵ of q and r approaches zero, then

$$\underset{\epsilon \to 0}{\text{Lt}} \int_\epsilon^y u\,dy - \tfrac{1}{2}\int_0^x q\,dx = 0 \tag{2.2a}$$

since $\int_B^A v\,dx$ equals half of the source flux from the x axis between B and r.

The velocity component u is given by $u = U + u_i$

where u_i is induced by the source distribution and is given by

$$u_i = \int_{a=0}^{1} \left\{ \frac{(x-a)}{(x-a)^2 + y^2} \right\} \frac{q(a)}{2\pi}\, da$$

Upon integration with respect to y it can be shown that

$$\int_{\epsilon}^{y} u_i \, dy = \int_0^1 \frac{q(a)}{2\pi} \left\{ \tan^{-1} \frac{y}{x-a} - \tan^{-1} \frac{\epsilon}{x-a} \right\} da$$

It then follows that

$$\underset{\epsilon \to 0}{\text{Lt}} \int_{\epsilon}^{y} u_i \, dy = \int_0^1 \frac{q(a)}{2} \tan^{-1} \frac{y}{x-a} \, da \qquad (2.3)$$

Where $\tan^{-1} \frac{y}{x-a}$ lies between $\pm \frac{\pi}{2}$

We now define

$$Q(x) + \int_0^x \frac{q(a)}{2\,U} \, da$$

Thus $Q(0) = 0$

$Q(1) = 0$

since $Q(1)$ is the total source strength which is zero for a closed profile.

In fact $Q(x)$ is an approximation to the y_d co-ordinate, equation (6), which has been evaluated in equation (10).

The integration in (2.3) is now carried out to give

$$\int_0^1 \frac{q(a)}{2\pi} \tan^{-1} \frac{y}{x-a} \, da$$

$$= UQ(x) - \frac{U}{\pi} \int_0^1 \frac{Q(a)\, y}{(x-a)^2+y^2} \, da$$

Finally equation (2.2)a becomes

$$1 - \frac{1}{\pi} \int_0^1 \frac{Q(a)}{(x-a)^2+y^2} \, da = 0 \qquad (2.4)$$

x,y in this equation are the profile streamline co-ordinates corresponding to the source distribution q(a). To determine the streamline, equation (2.4) was integrated numerically for several values of y at chosen x positions, the correct value of y being finally obtained by interpolation.

Leading edge co-ordinate

There is no reason to expect that the profile streamline stagnation point will occur at x = 0. It is more likely to be slightly upstream of this point. At the nose we have, since y = 0

$$\pi = \int_0 \frac{Q(a)}{(x - a)^2} \, da$$

It can be shown that this reduces with good approximation to

$$\sqrt{-x} = \frac{B_o}{1+3B_o-B_2-B_3} - \frac{5B_o-4B_2-6B_3}{1+3B_o - B_2 - B_3} \, x \qquad (2.5)$$

the second term in fact being negligible. For the profile considered here this gave, referring to Figure (13), the value

$$B_p = .005$$

FIG.1

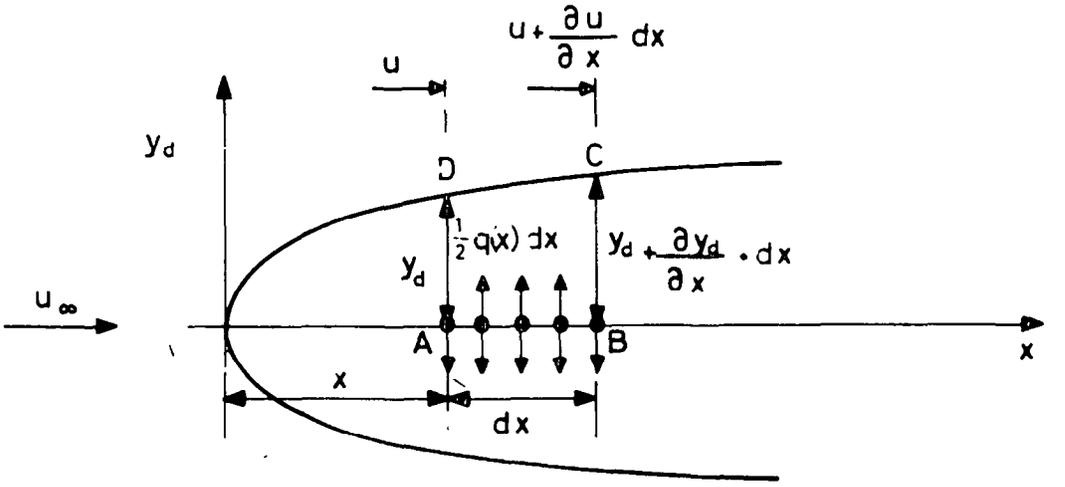

FIG 1(a) PROFILE THICKNESS

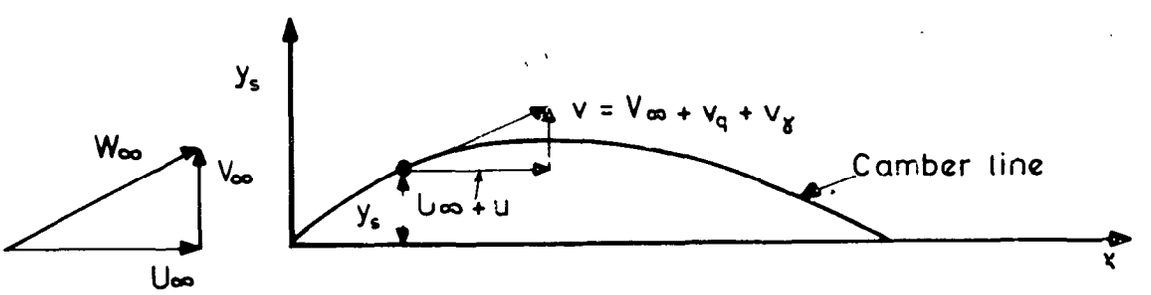

FIG 1 (b) CAMBER DISTRIBUTION

DIAGRAMS FOR DERIVATION OF SCHLICHTINGS KINEMATIC FLOW EQUATIONS

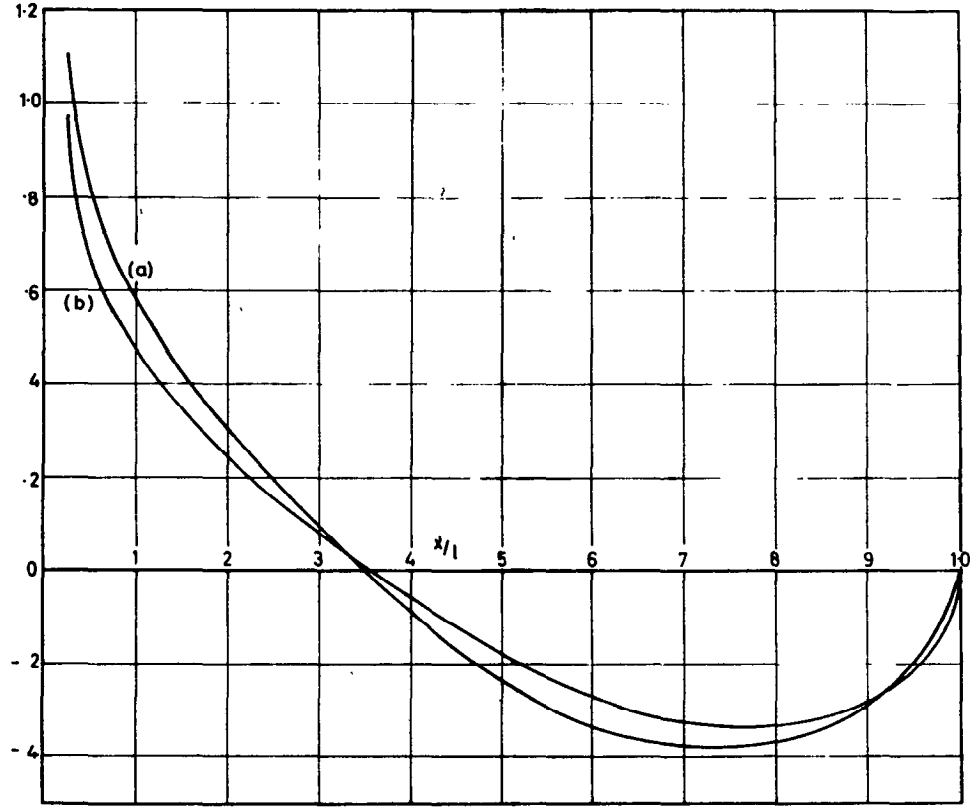

$\frac{q(x)}{U_\infty}$

FIG. 2

CURVE (a) EXACT THEORY

B_0 = 0·081307

B_2 = 0 111628

B_3 = 0 035256

CURVE (b) APPROXIMATE THEORY

B_0 = 0 072546

B_2 = 0 093271

B_3 = 0 013467

COMPARISON OF SOURCE DISTRIBUTIONS TO REPRESENT A GIVEN AEROFOIL

FIG. 3

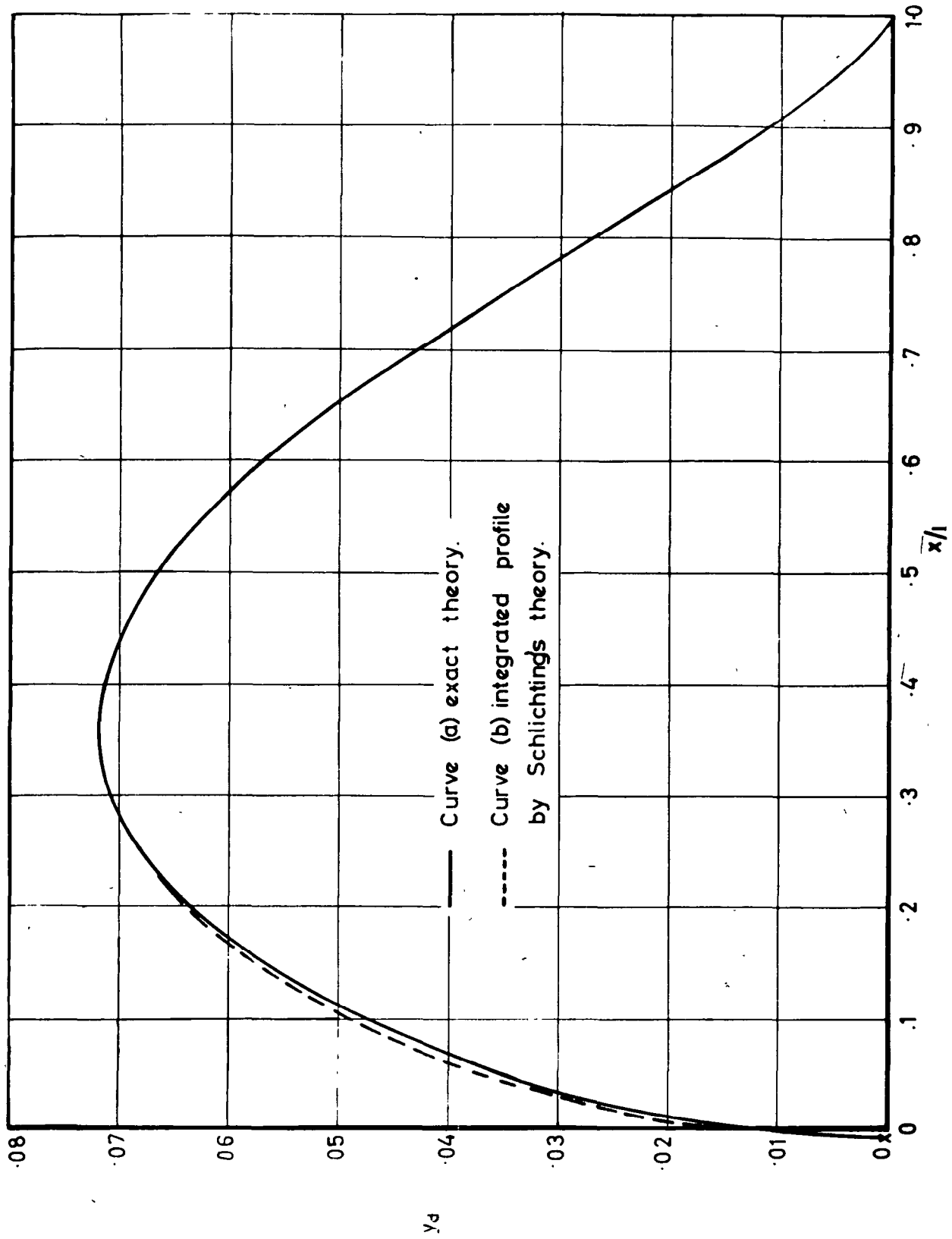

COMPARISON OF PROFILE GIVEN BY EXACT THEORY WITH THE INTEGRATED PROFILE BY SCHLICHTING'S METHOD OF ANALYSIS

FIG.4

Curve (a) exact theory.

Curve (b) Schlichting's theory.

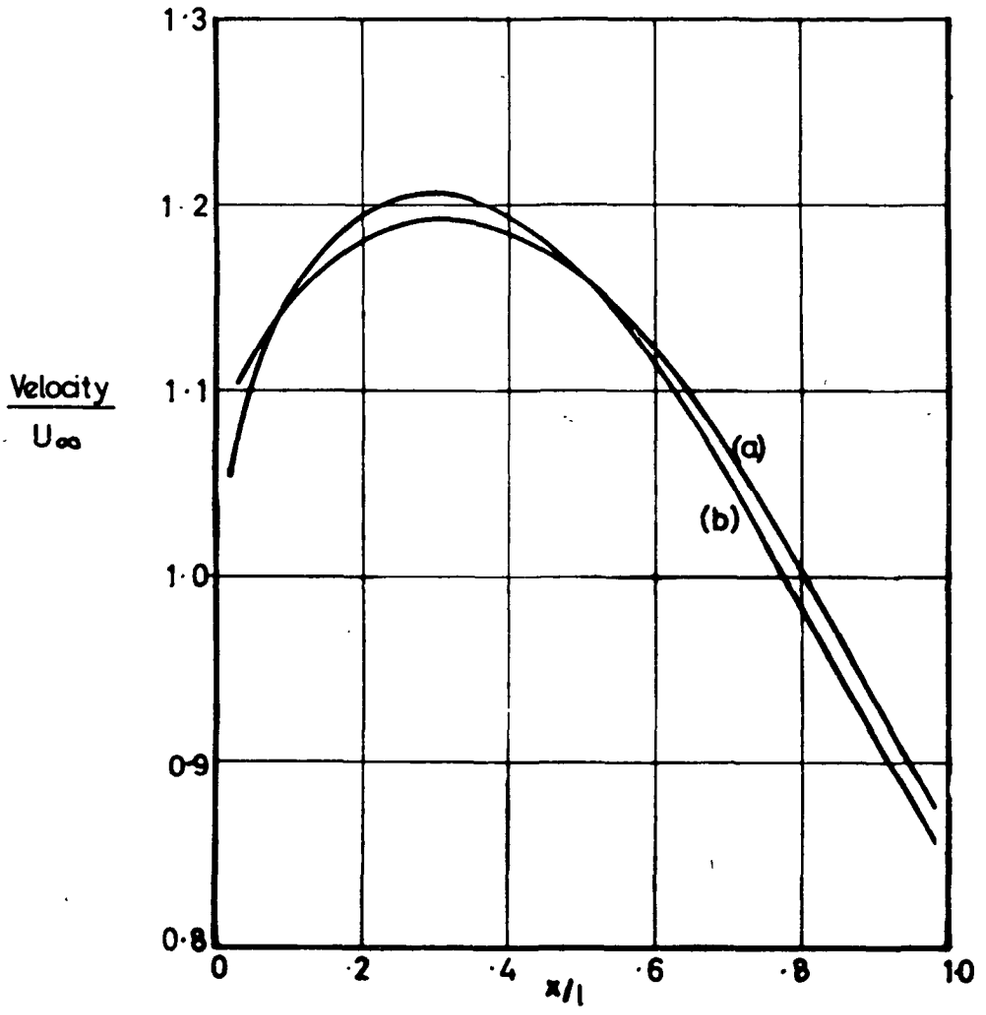

PROFILE SURFACE VELOCITY BY EXACT AND APPROXIMATE THEORIES.

FIG. 5

$$P = \frac{p - p_\infty}{\frac{1}{2} \rho U_\infty^2}$$

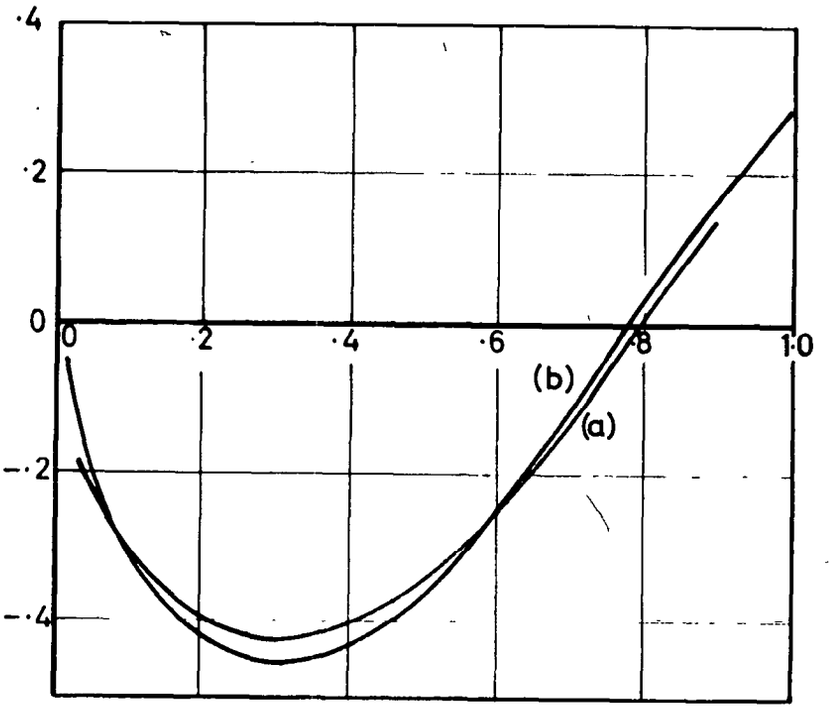

Curve (a) exact theory

Curve (b) Schlichting's approximate theory.

SURACE PRESSURE DISTRIBUTION
BY EXACT AND APPROXIMATE THEORIES.

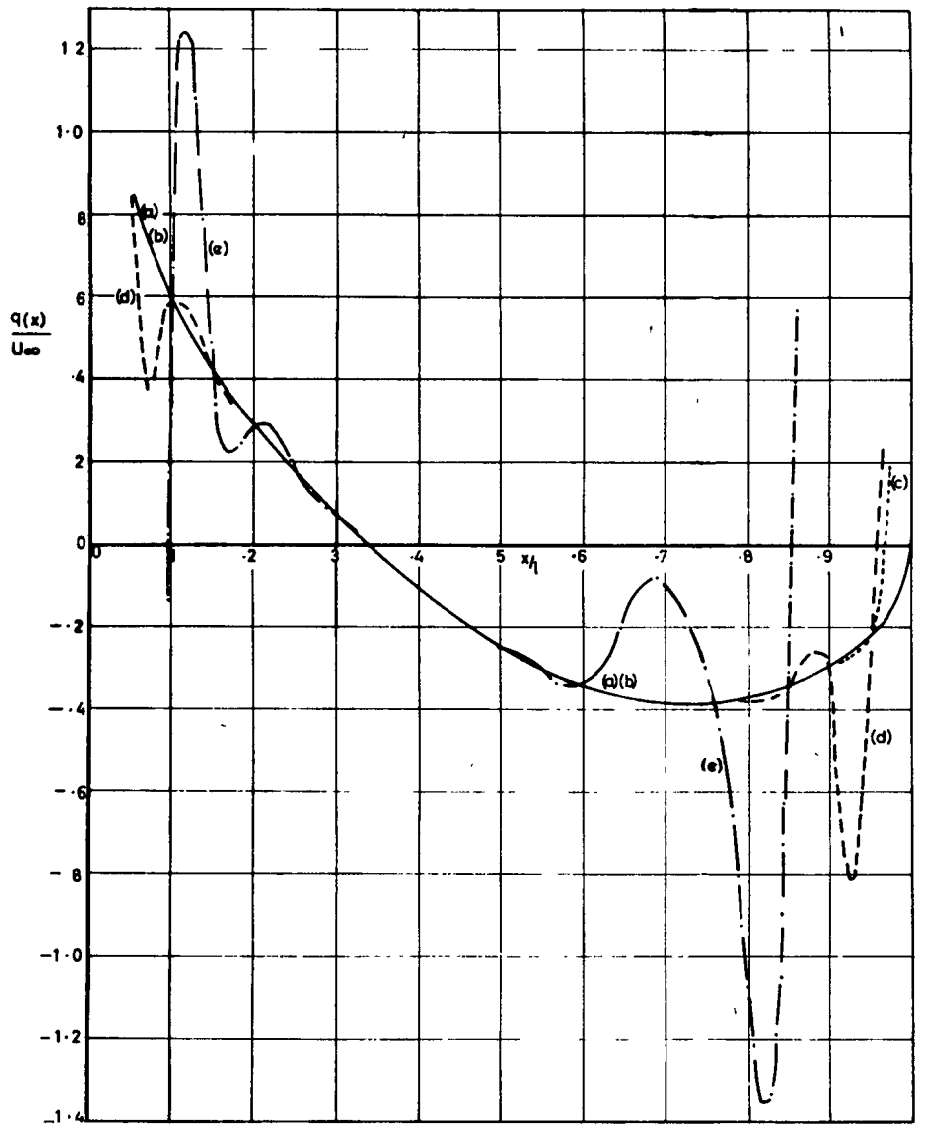

(a) Original singularity distribution

—— (b) Singularity distribution for 19 control points with data to 8 significant figures

----- (c) 19 control points, 4 significant figures

– – – (d) 19 control points, 3 significant figures

—·— (e) Profile with bulge

FIG.6

INFLUENCE OF PROFILE DATA ACCURACY & SMOOTHNESS UPON DERIVED SINGULARITY DISTRIBUTION

FIG. 7

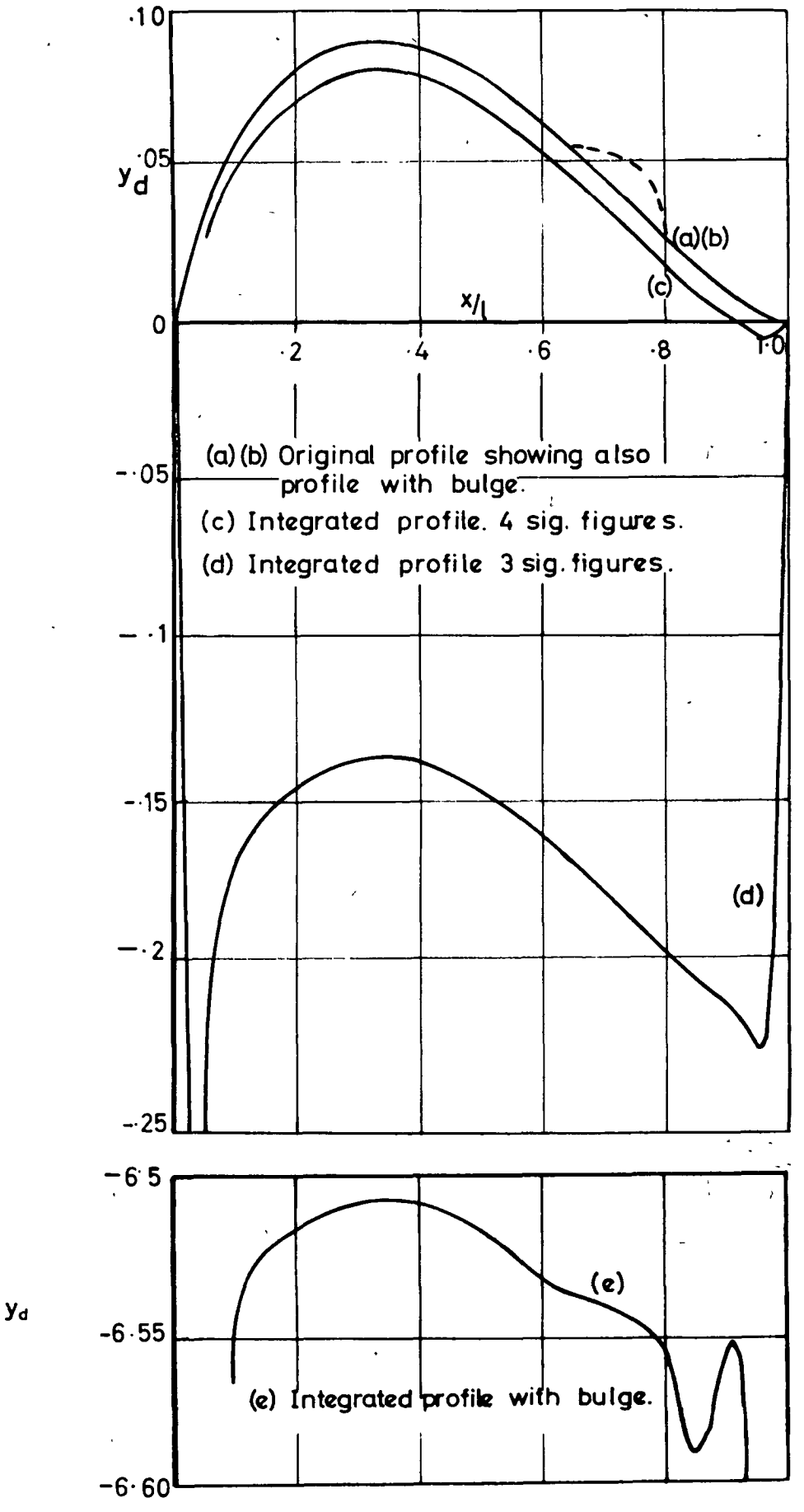

INTEGRATED PROFILES FOR SINGULARITY STRENGTHS SHOWN IN FIGURE 6.

FIG.8

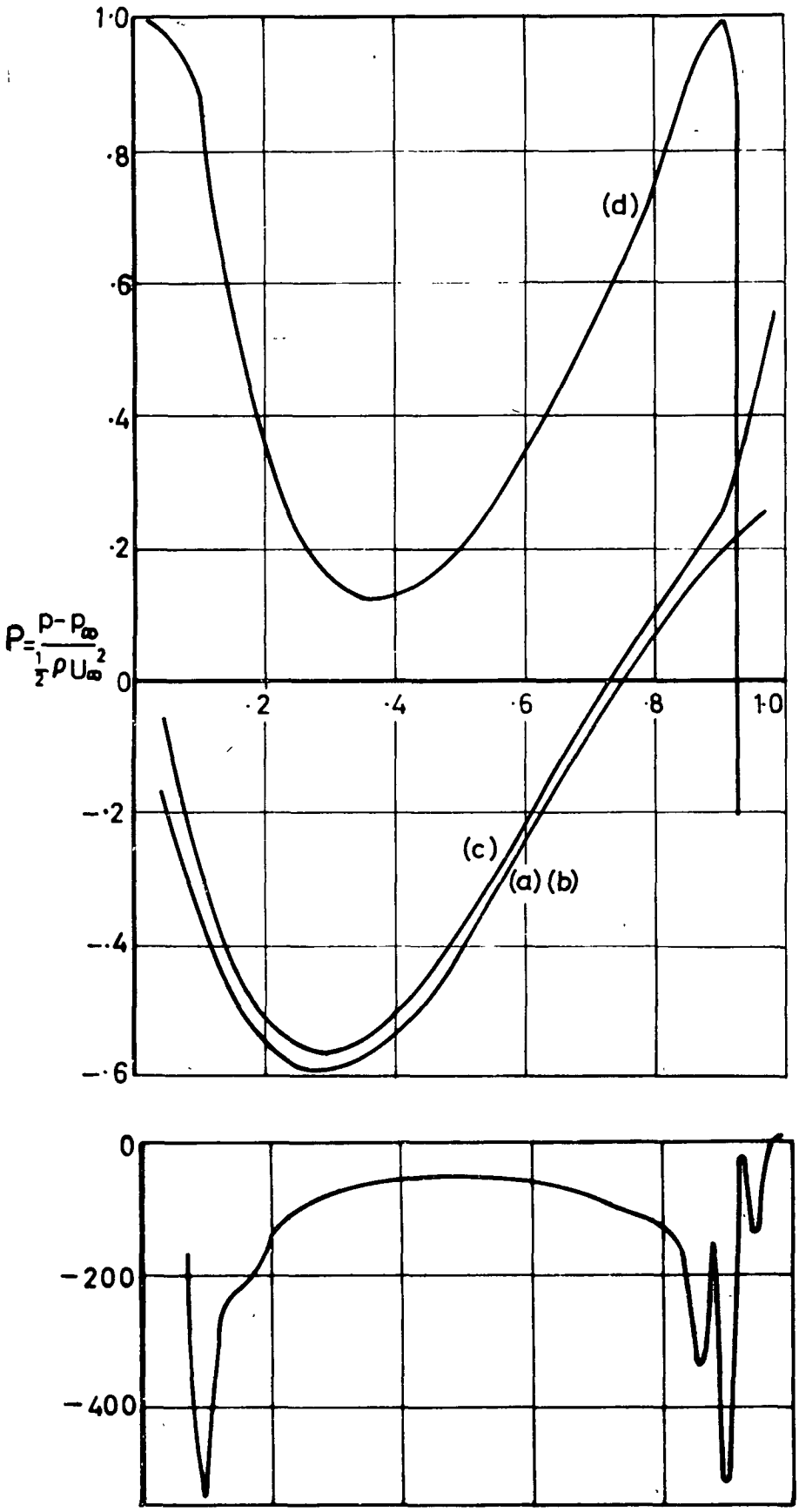

(a)(b) Original profile 8 sig. figures.

(c) 4 sig. figures.

(d) 3 sig figures.

(e) Profile with bulge.

COMPUTED PRESSURE DISTRIBUTIONS FOR DERIVED SINGULARITY STRENGTHS SHOWN IN FIGURE (6)- 19 CONTROL POINTS.

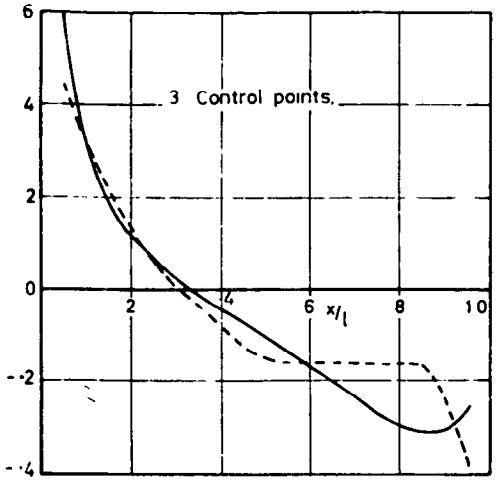

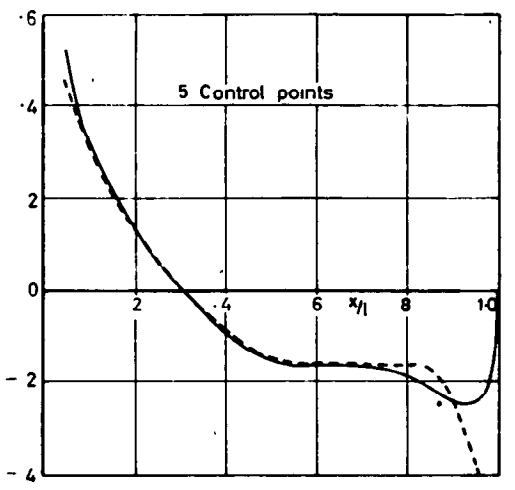

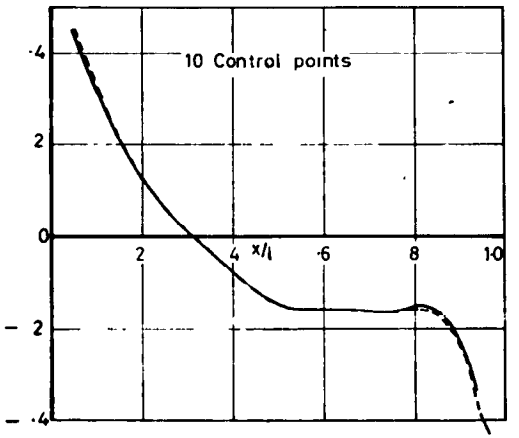

Dashed curve shows y_d' for original profile.
Equation (6) states approximately

$$y_d' = \frac{q(x)}{2U_\infty}$$

FIG 9

MATCHING OF PROFILE SLOPE WITH 3, 5 AND 10 CONTROL POINTS

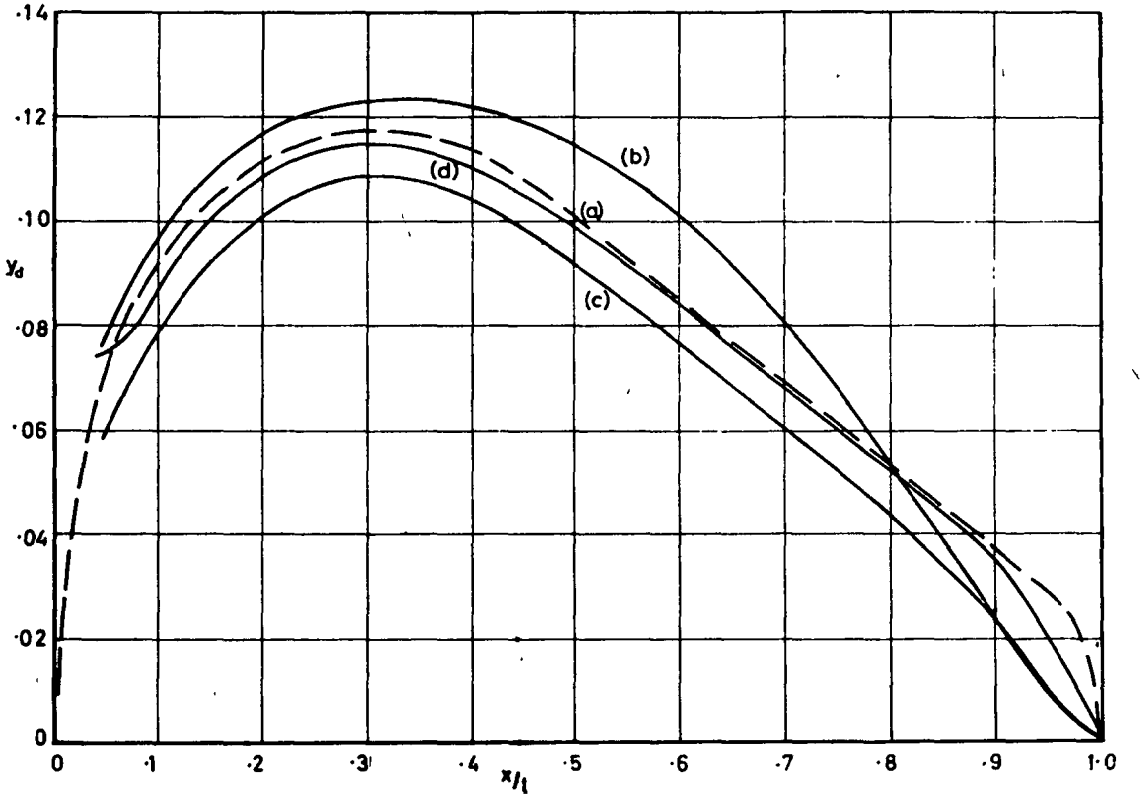

(a) Original profile.

(b) 3 Control points.

(c) 5 Control points.

(d) 10 Control points

FIG.10

INTEGRATED PROFILES USING 3, 5 AND 10 CONTROL POINTS.

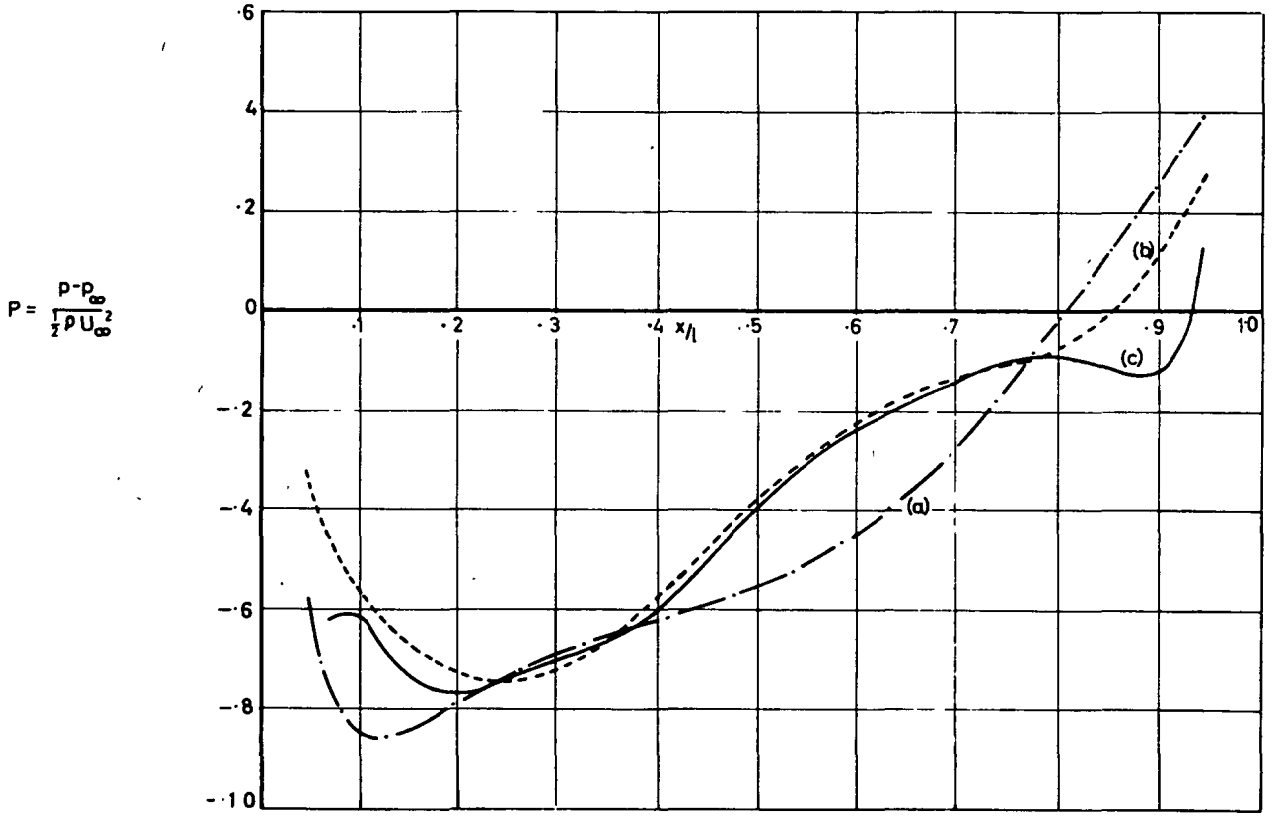

(a) 3 Control points
(b) 5 Control points
(c) 10 Control points

FIG. 11

COMPUTED PRESSURE DISTRIBUTIONS FOR PROFILE MATCHED AT 3,5 AND 10 CONTROL POINTS.

FIG.12

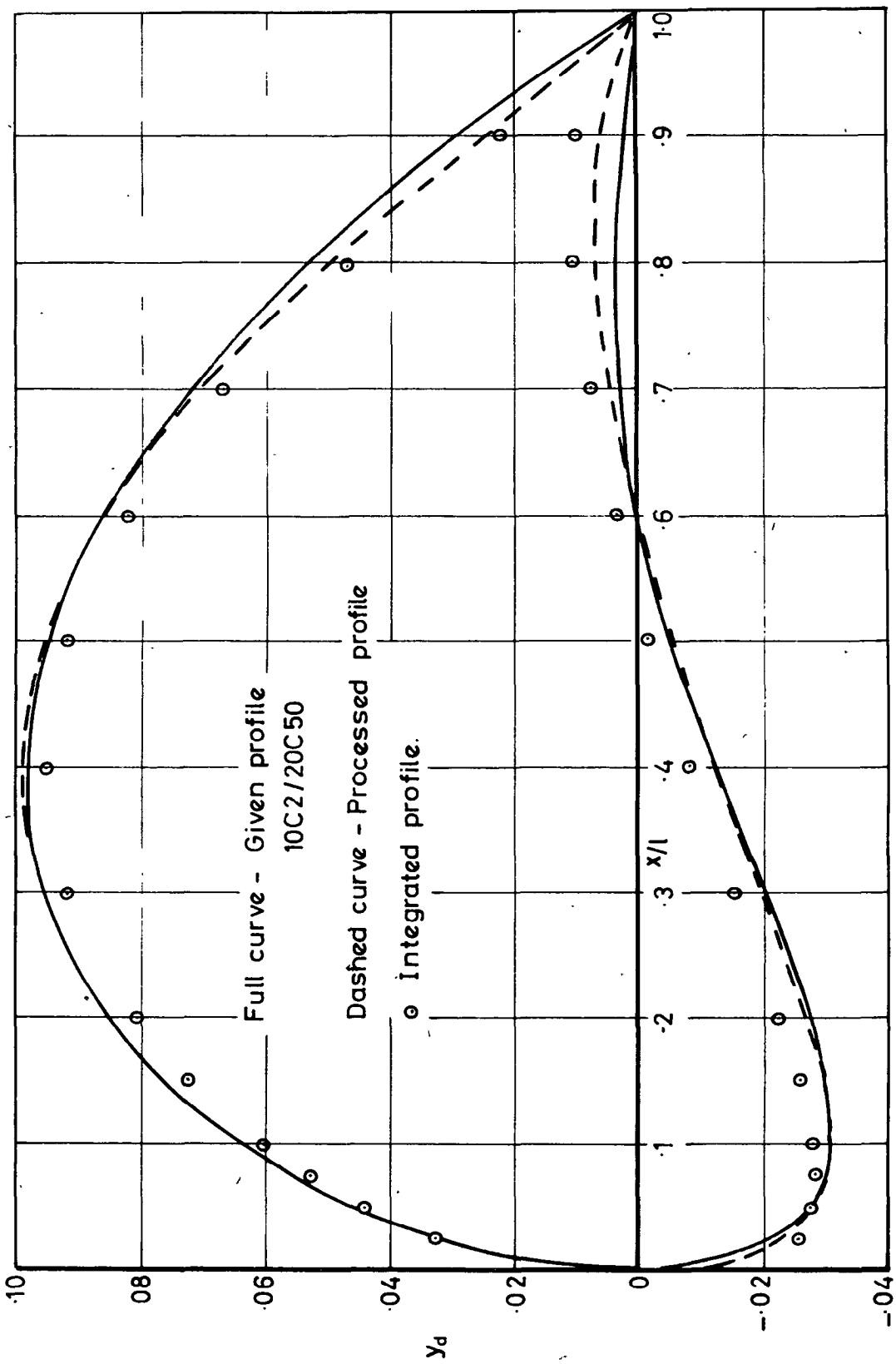

COMPARISON BETWEEN ORIGINAL, PROCESSED AND FINAL INTEGRATED PROFILES FOR A COMPRESSOR CASCADE 10C2/20C50 WITH 56·8° STAGGER AND 1·175 SOLIDITY.

FIG.13

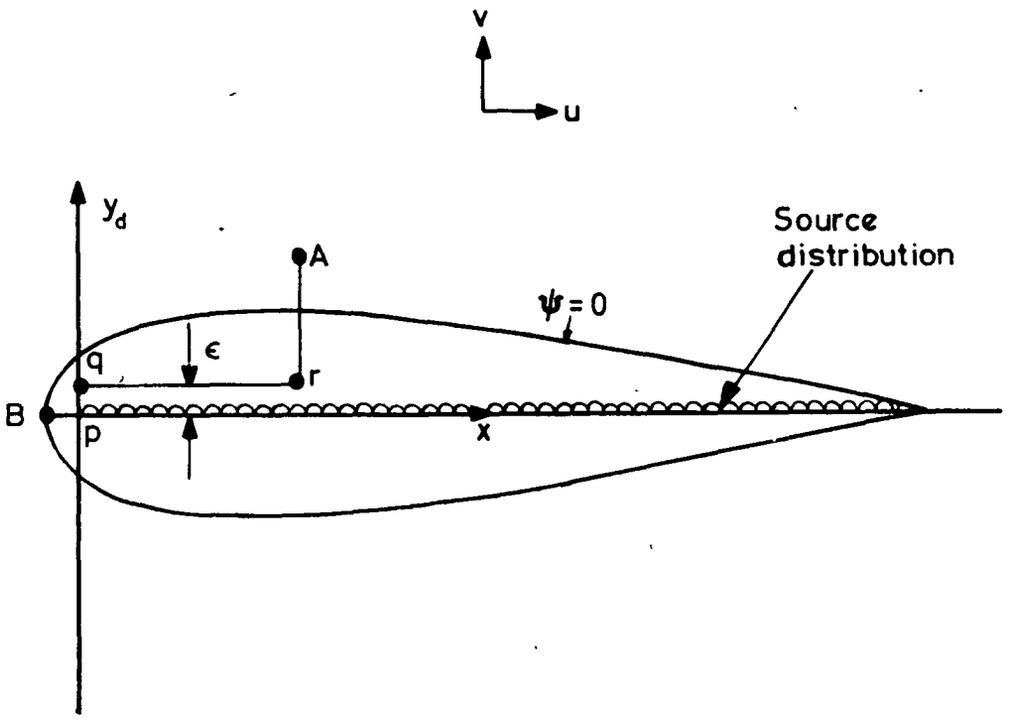

DERIVATION OF PROFILE INDUCED BY SOURCE DISTRIBUTION.

FIG.14

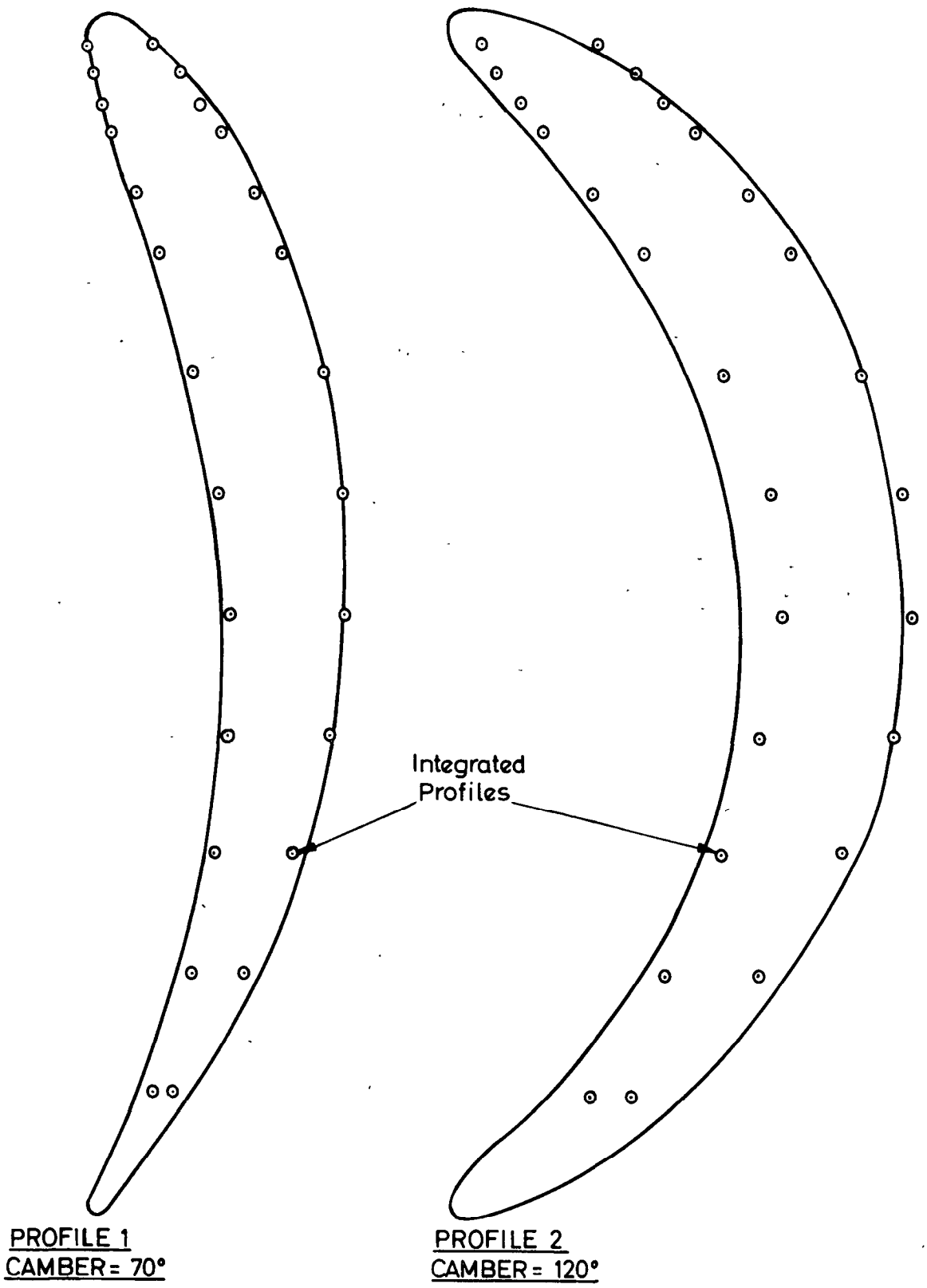

HIGH CAMBERED PROFILES COMPARED WITH MATCHING PROFILES INTEGRATED FROM SCHLICHTING'S ANALYSIS

FIG.15

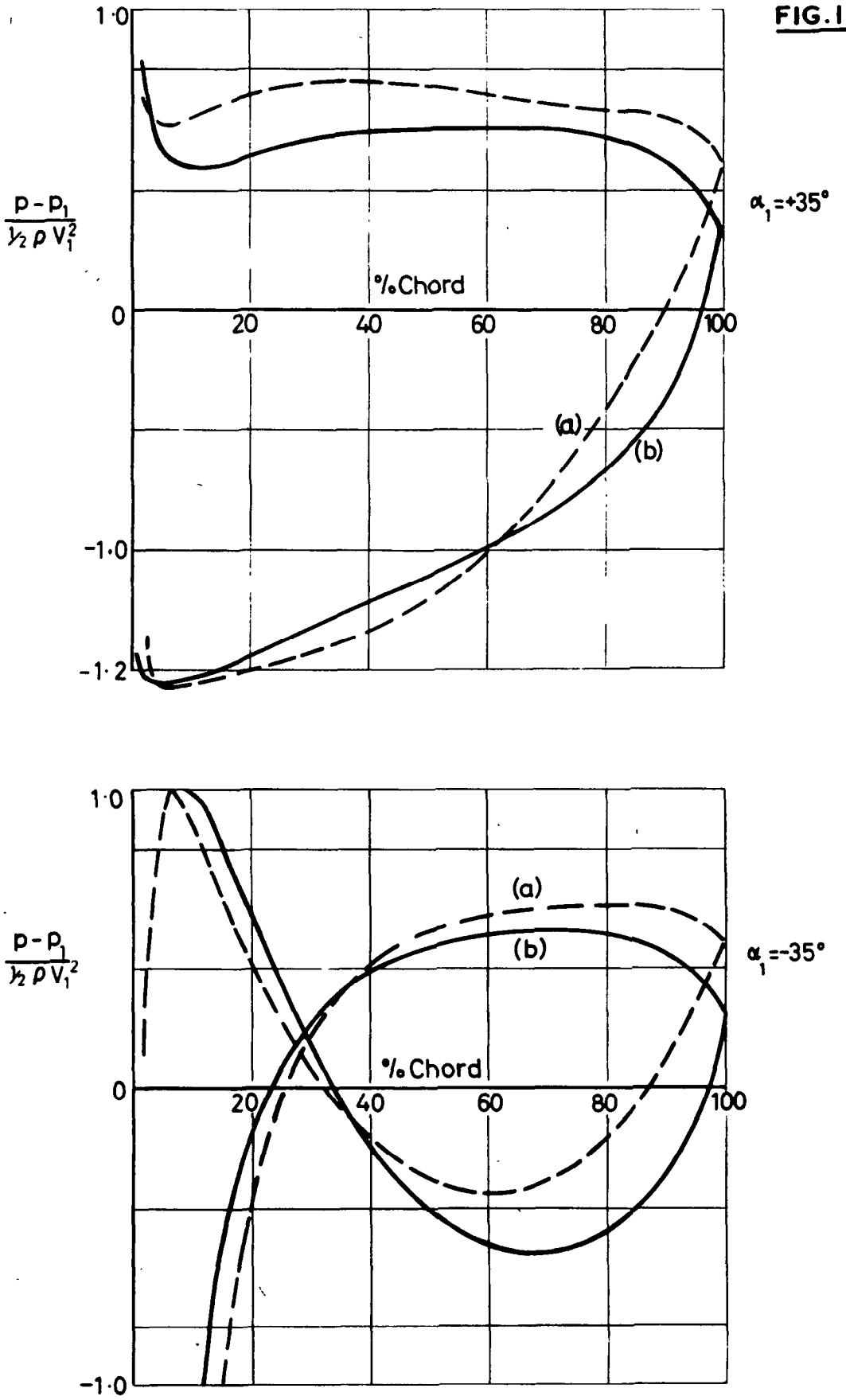

COMPARISON OF PREDICTED PRESSURE DISTRIBUTIONS FOR A 70° CAMBER CASCADE APPROXIMATING TO 10C4/70C50 AT ZERO STAGGER ACCORDING TO
(a) SCHLICHTING'S APPROXIMATE THEORY
(b) EXACT THEORY OF MERCHANT & COLLAR

FIG 16

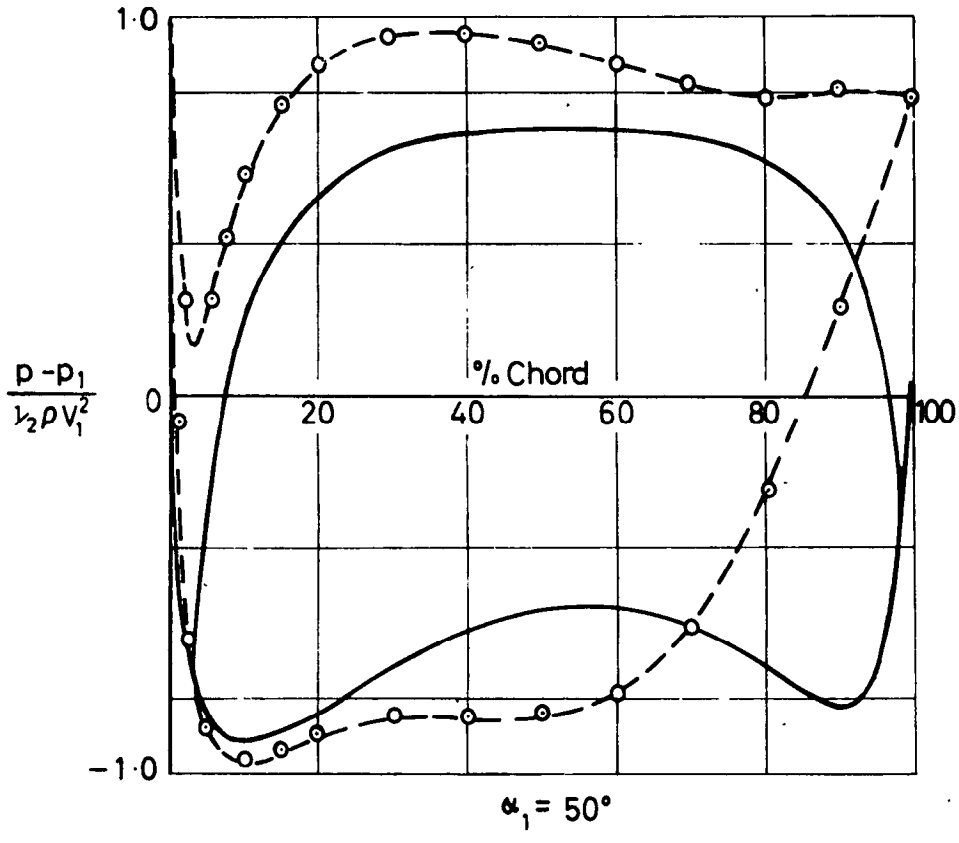

COMPARISON OF ANALYSIS OF A 120° CAMBER PROFILE BY MERCHANT & COLLAR'S EXACT THEORY AND BY SCHLICHTING'S THEORY

A.R.C. C.P. No. 813
September, 1964
R. I. Lewis and G. A. Pennington

THEORETICAL INVESTIGATION OF SOME BASIC ASSUMPTIONS OF SCHLICHTING'S SINGULARITY METHOD OF CASCADE ANAYYSIS

The accuracy of Schlichting's kinematic source flow equation has been investigated for an isolated symmetrical aerofoil. Studies are presented also of the suitability of the Glauert series for representing profiles by source/vortex distributions. Influence of data rounding off error upon profile analysis with large numbers of control points has been examined, and importance of data accuracy and smoothness stressed. An estimation of the optimum number of control points has been made for a typical profile. A method of initial data processing to ensure a valid computation has been suggested.

A.R.C. C.P. No. 813
September, 1964
R. I. Lewis and G. A. Pennington

THEORETICAL INVESTIGATION OF SOME BASIC ASSUMPTIONS OF SCHLICHTING'S SINGULARITY METHOD OF CASCADE ANALYSIS

The accuracy of Schlichting's kinematic source flow equation has been investigated for an isolated symmetrical aerofoil. Studies are presented also of the suitability of the Glauert series for representing profiles by source/vortex distributions. Influence of data rounding off error upon profile analysis with large numbers of control points has been examined, and importance of data accuracy and smoothness stressed. An estimation of the optimum number of control points has been made for a typical profile. A method of initial data processing to ensure a valid computation has been suggested.

A.R.C. C.P. No. 813
September, 1964
R. I. Lewis and G. A. Pennington

THEORETICAL INVESTIGATION OF SOME BASIC ASSUMPTIONS OF SCHLICHTING'S SINGULARITY METHOD OF CASCADE ANALYSIS

The accuracy of Schlichting's kinematic source flow equation has been investigated for an isolated symmetrical aerofoil. Studies are presented also of the suitability of the Glauert series for representing profiles by source/vortex distributions. Influence of data rounding off error upon profile analysis with large numbers of control points has been examined, and importance of data accuracy and smoothness stressed. An estimation of the optimum number of control points has been made for a typical profile. A method of initial date processing to ensure a valid computation has been suggested.

Printed and published by
HER MAJESTY'S STATIONERY OFFICE

To be purchased from
York House, Kingsway, London w.c.2
423 Oxford Street, London w.1
13A Castle Street, Edinburgh 2
109 St. Mary Street, Cardiff
39 King Street, Manchester 2
50 Fairfax Street, Bristol 1
35 Smallbrook, Ringway, Birmingham 5
80 Chichester Street, Belfast 1
or through any bookseller

Printed in England

C.P. No. 813

S.O. Code No. 23-9016-13